Supporting Information

Tailoring Electronegativity of Bimetallic Ni/Fe Metal-Organic Framework Nanosheets for Electrocatalytic Water Oxidation

Meihui Ying[a,b,c], Rui Tang[d], Wenjie Yang[a], Weibin Liang[a], Guizeng Yang[b], Haibo Pan[b], Xiaozhou Liao[c], Jun Huang[a]**

[a] Laboratory for Catalysis Engineering, School of Chemical and Biomolecular Engineering, Sydney Nano Institute, The University of Sydney, Sydney, New South Wales 2006, Australia

[b] College of Chemistry, Qishan Campus, Fuzhou University, Fuzhou, Fujian 350108, P. R. China

[c] School of Aerospace, Mechanical and Mechatronic Engineering, Sydney Nano Institute, The University of Sydney, Sydney, New South Wales 2006, Australia

[d] School of Physics, Sydney Nano Institute, The University of Sydney, Sydney, New South Wales 2006, Australia

Corresponding Author

*Email: jun.huang@sydney.edu.au, hbpan@fzu.edu.cn

Supporting text

Calculation of the specific current density and resistance values in Figure S7: Taking the current density values of $Ni_{0.6}$Fe-MIL-88A/NF as reference data, $j_{0.7}/j_{0.6}$ means the current density values of $Ni_{0.7}$Fe-MIL-88A/NF divided by that of $Ni_{0.6}$Fe-MIL-88A/NF, and $R_{0.7}/R_{0.6}$ means the resistance values of $Ni_{0.7}$Fe-MIL-88A/NF divided by that of $Ni_{0.6}$Fe-MIL-88A/NF.

Calculation of systematic geometric mean electronegativity: In this study, the calculation model of Ni_xFe-MIL-88A/NF is represented by 100 M_3O cluster (Scheme below).

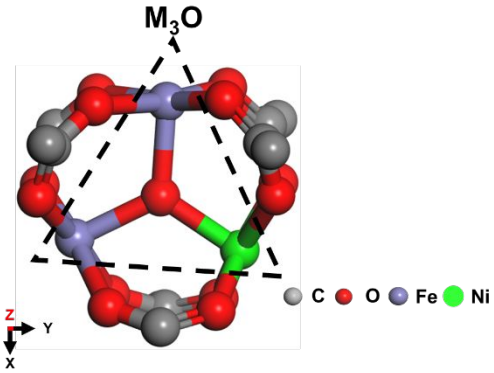

NiFe cluster of NiFe-MIL-88A

The ionic electronegativity (IE) values of Ni^{2+}, Fe^{3+} and O are 1.361, 1.651 and 3.44, respectively. (detailed calculations can be found in the studies of the Xue group) [1] Taking the calculation of the systematic geometric mean electronegativity value for $Ni_{0.6}$Fe-MIL-88A/NF as an example:
For $Ni_{0.6}$Fe-MIL-88A, 100 M_3O means 400 atoms which contains 6/16*300 Ni (112.5), 10/16*300 Fe (187.5) and 100 O.
Systematic geometric mean electronegativity of $Ni_{0.6}$Fe-MIL-88A/NF

$$= \sqrt[400]{1.361^{112.5} * 1.651^{187.5} * 3.44^{100}}$$

$$= 1.8787$$

The systematic geometric mean electronegativity values of Ni_xFe-MIL-88A/NF are listed in Table S3.

Supporting figures and tables

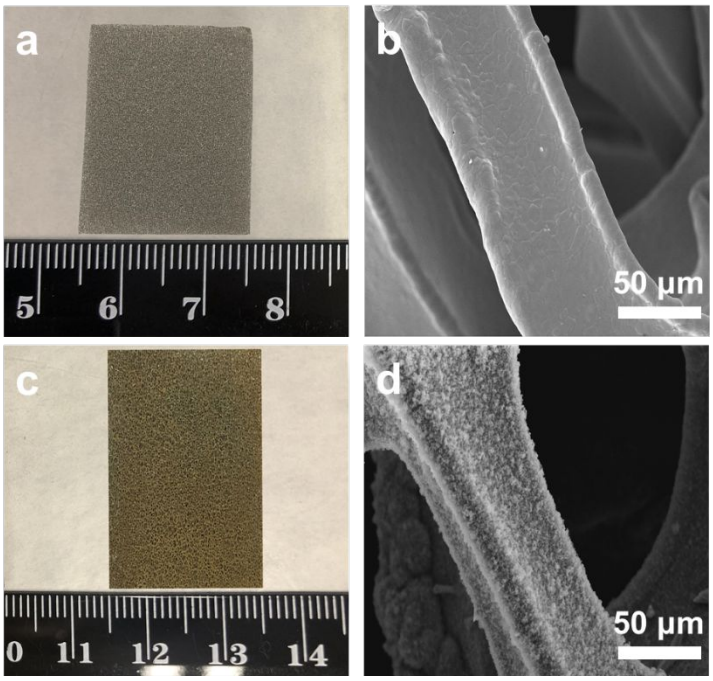

Figure S1 (a) An optical image and (b) SEM image of Bare NF, (c) An optical image and (d) SEM image of NiFe-MIL-88A/NF.

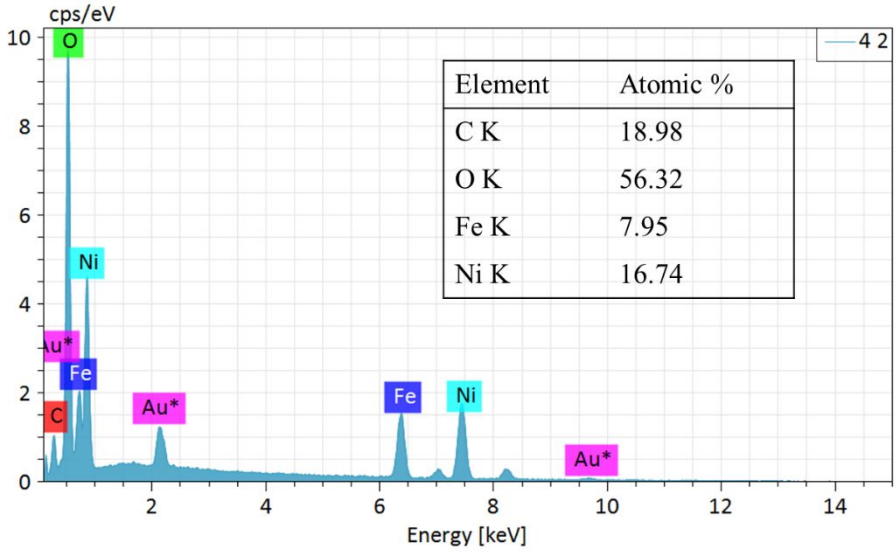

Figure S2 EDS spectrum of NiFe-MIL-88A/NF.

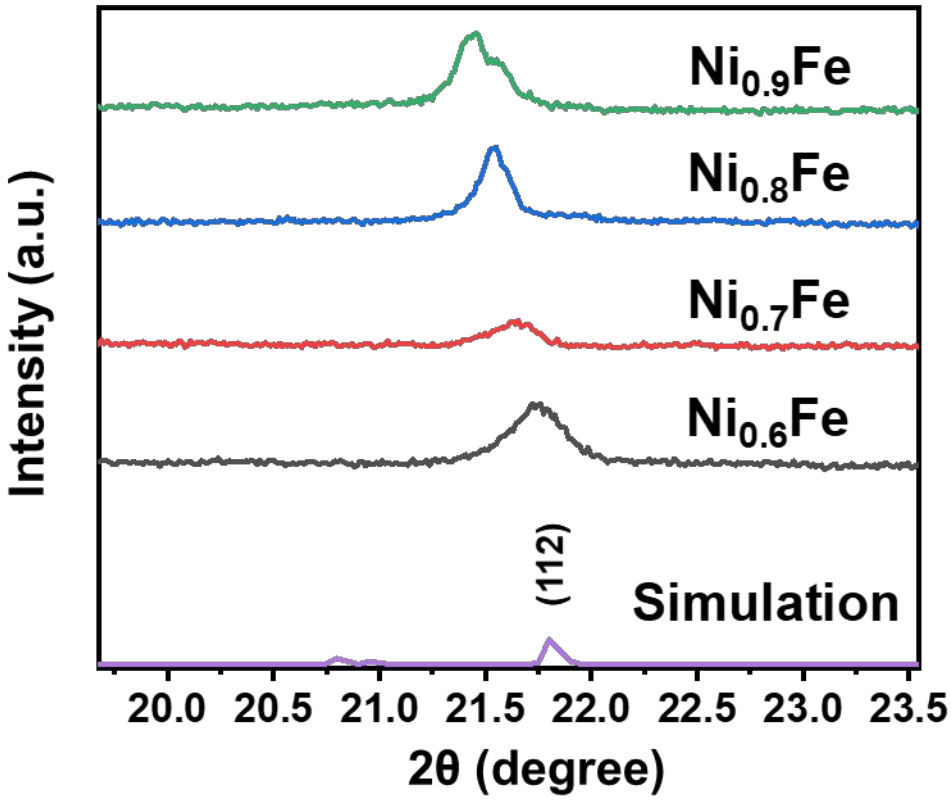

Figure S3 XRD patterns of the enlarged view of (112) for Ni_xFe-MIL-88A/NF.

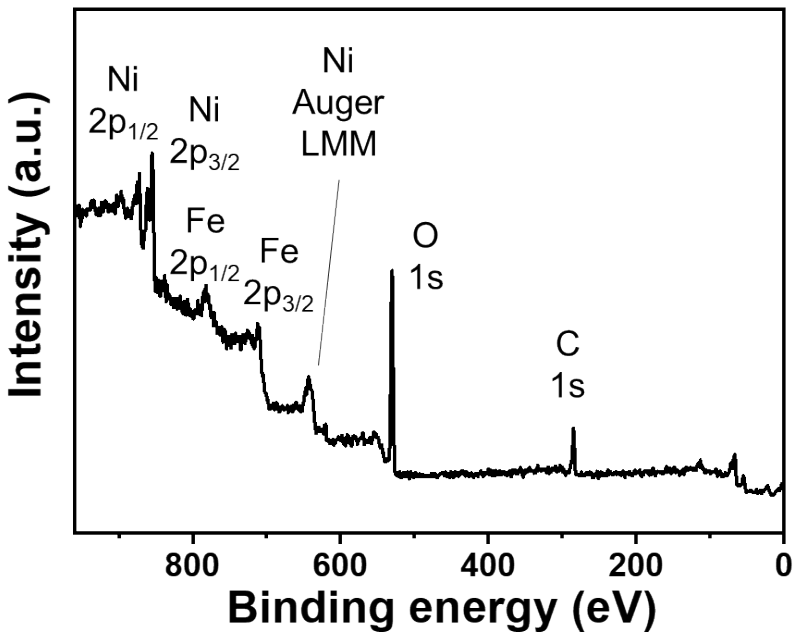

Figure S4 XPS survey spectrum of NiFe-MIL-88A/NF.

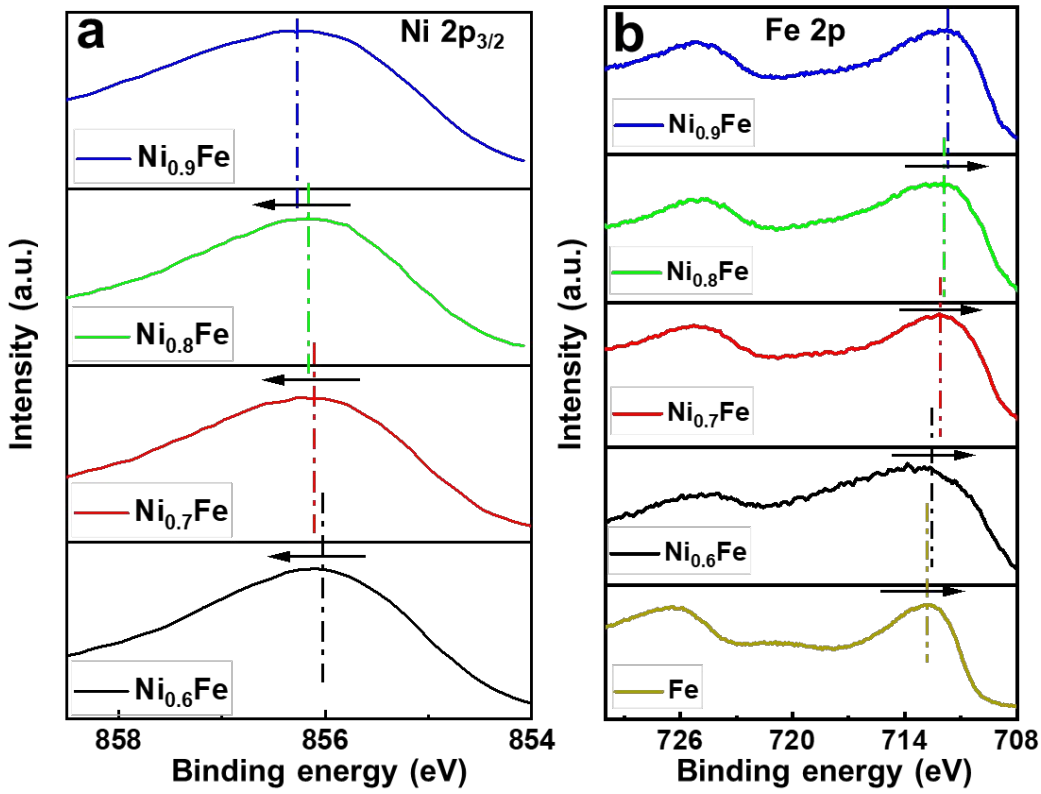

Figure S5 (a) The Ni $2p_{3/2}$, and (b) Fe 2p XPS spectra of Fe-MIL-88A, $Ni_{0.6}$Fe-MIL-88A/NF, $Ni_{0.7}$Fe-MIL-88A/NF, $Ni_{0.8}$Fe-MIL-88A/NF, and $Ni_{0.9}$Fe-MIL-88A/NF.

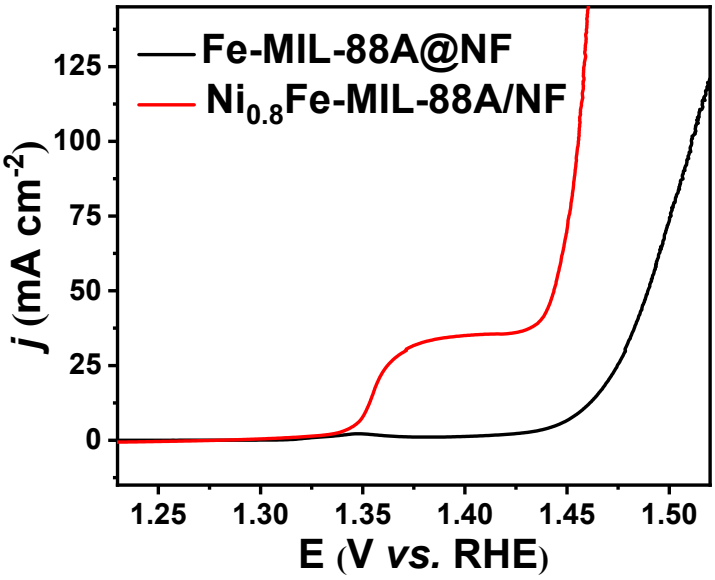

Figure S6 The LSV plots of $Ni_{0.8}$Fe-MIL-88A/NF and Fe-MIL-88A@NF.

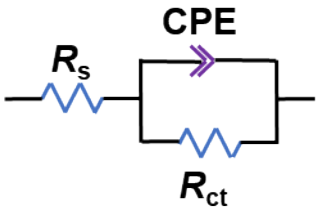

Figure S7 The equivalent circuit diagram, while Rs is the resistance of solution, R_{ct} is the charge transfer resistance at the catalyst/solution interface, and CPE is the constant phase angle element.

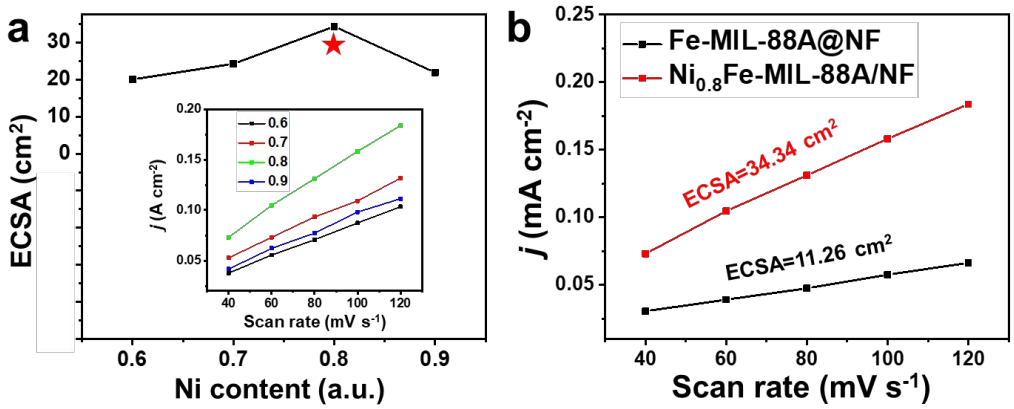

Figure S8 a) Calculated ESCA value (inset: Current density at 1.11 V vs the different scan rate) of $Ni_{0.6}$Fe-MIL-88A/NF, $Ni_{0.7}$Fe-MIL-88A/NF, $Ni_{0.8}$Fe-MIL-88A/NF, and $Ni_{0.9}$Fe-MIL-88A/NF. (b) Current density at 1.11 V vs the scan rate of $Ni_{0.8}$Fe-MIL-88A/NF and Fe-MIL-88A@NF.

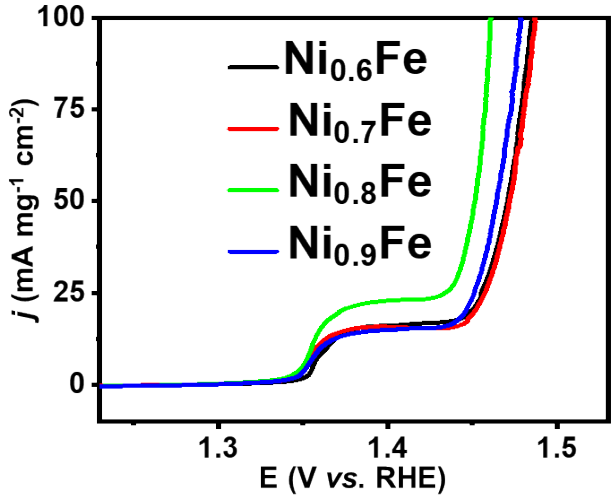

Figure S9 the LSV plots of the current densities corrected by mass loading of Ni_xFe-MIL-88A/NF at a potential of 1.46 V.

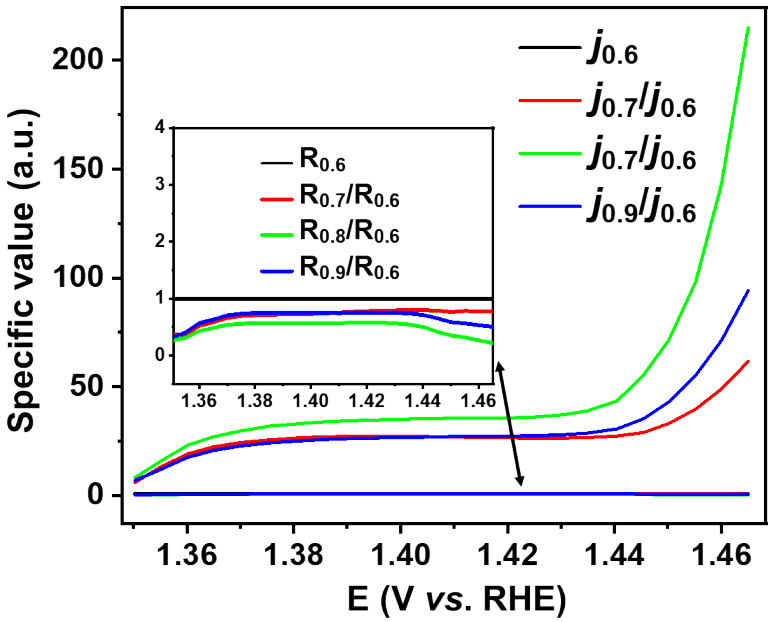

Figure S10 The specific values of current density and resistance (inset), respectively, with different potential values for Ni_xFe-MIL-88A/NF (The values of $Ni_{0.6}Fe$-MIL-88A/NF is the benchmark value).

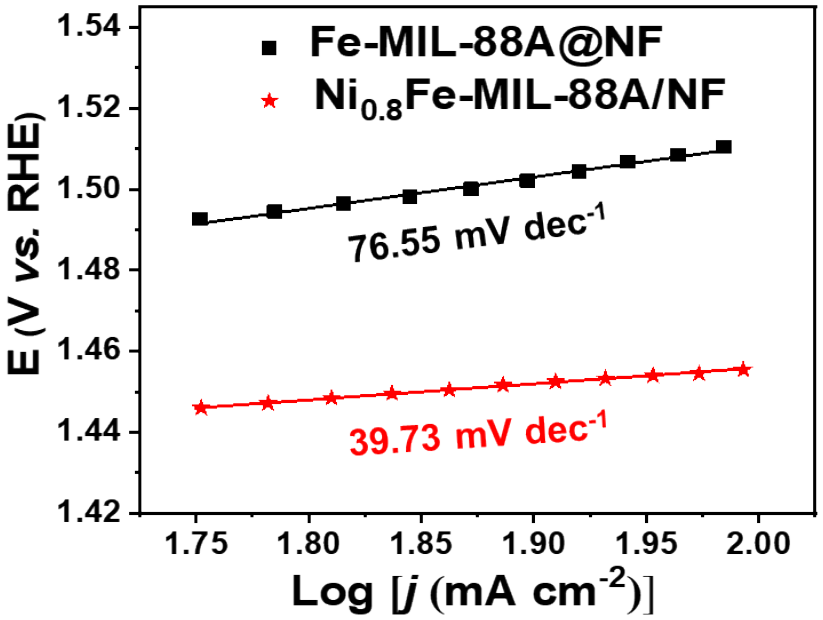

Figure S11 The Tafel slopes of $Ni_{0.8}$Fe-MIL-88A/NF and Fe-MIL-88A@NF.

Table S1 Ni content in the surface layer of the four kinds of Ni_xFe-MIL-88A/NF samples determined by the deviation from the stoichiometry ratio with XPS

Sample	Element	Area (P) CPS.eV	Sensitivity factor (SF)	P/SF	Ni content
$Ni_{0.6}Fe$-MIL-88A/NF	Ni $2p_{3/2}$	49659.04	22.18	2238.91	0.6
	Fe $2p_{3/2}$	60986.55	16.42	3714.16	
$Ni_{0.7}Fe$-MIL-88A/NF	Ni $2p_{3/2}$	52440.35	22.18	2364.31	0.7
	Fe $2p_{3/2}$	53008.97	16.42	3228.32	
$Ni_{0.8}Fe$-MIL-88A/NF	Ni $2p_{3/2}$	68766.39	22.18	3100.38	0.8
	Fe $2p_{3/2}$	63703.33	16.42	3879.62	
$Ni_{0.9}Fe$-MIL-88A/NF	Ni $2p_{3/2}$	59039.5	22.18	2661.83	0.9
	Fe $2p_{3/2}$	50045.83	16.42	3047.86	

Table S2 OER performance of MOFs based electrocatalysts in-situ grown on NF: this work vs. literature

Sample	Overpotential (mV, η=50 mA/cm^2)	Tafel slope (mV/dec)	Reference
This work	213	39.7	This work
HP-CoP NA/NF	330	91.7	[2]
Ni_2P-Co_2P@C/NF	290	64	[3]
$Ni_{0.5}Fe_{0.5}$-HP	360	79	[4]
NiFeZn-MNS/NF	308	49	[5]
CoNi-NDC/PANI-NF	370	73.3	[6]
Co_3O_4 /MoS_2	295	45	[7]
Fe_5Ni (BDC)(DMF,F)/NF	220	37.4	[8]
FeNi MFN-MOFs(2:1)/NF	235	55.4	[9]
NF@Fe_2−Ni_2P/C	430@500 mA cm^{-2}	26	[10]
Fe-MOF/NF	370	72	[11]
Fe(II)-MOF-74 NAs@NF	235	41.1	[12]
$Fe_{0.1}$-Ni-MOF/NF	243	69.8	[13]
NiCo-MOF/LDH/NF	300@100 mA cm^{-2}	106	[14]
FeNi NFN-MOF/NF	295	58.8	[15]
Cu_3P@C-120	395@30 mA cm^{-2}	24	[16]
MIL-53(FeNi)/NF	233	31.3	[17]
NiFe MOF/NF	270	34	[18]

Table S3 The calculation detail of geometric mean electronegativity of 100 M_3O cluster for Ni_xFe-MIL-88A/NF.

Sample	Geometric mean electronegativity
Fe-MIL-88A/NF	1.98
$Ni_{0.6}Fe$-MIL-88A/NF	1.88
$Ni_{0.7}Fe$-MIL-88A/NF	1.87
$Ni_{0.8}Fe$-MIL-88A/NF	1.86
$Ni_{0.9}Fe$-MIL-88A/NF	1.85

Table S4 Ion concentration of iron and nickel in electrolyte after the long-time electrolysis process at 250 mA cm^{-2} in the presence of $Ni_{0.8}$Fe-MIL-88A/NF.

Iron ion concentration (mol/L)	%RSD[a] (iron)	Nickel ion concentration (mol/L)	%RSD (nickel)
1.23×10^{-7}	126.7	8.65×10^{-7}	223.2

[a]: RSD is related to the relative standard deviation.

References

1. Li, K.; Xue, D., Estimation of Electronegativity Values of Elements in Different Valence States. *J. Phys. Chem. A* **2006,** *110* (39), 11332-11337.
2. Wang, H.; Li, Y.; Wang, R.; He, B.; Gong, Y., Metal-organic-framework template-derived hierarchical porous CoP arrays for energy-saving overall water splitting. *Electrochim. Acta* **2018,** *284*, 504-512.
3. Zhou, Q.; Wang, J.; Guo, F.; Li, H.; Zhou, M.; Qian, J.; Li, T.-T.; Zheng, Y.-Q., Self-supported bimetallic phosphide-carbon nanostructures derived from metal-organic frameworks as bifunctional catalysts for highly efficient water splitting. *Electrochim. Acta* **2019,** *318*, 244-251.
4. Qiao, H.; Yang, Y.; Dai, X.; Zhao, H.; Yong, J.; Yu, L.; Luan, X.; Cui, M.; Zhang, X.; Huang, X., Amorphous (Fe)Ni-MOF-derived hollow (bi)metal/oxide@N-graphene polyhedron as effectively bifunctional catalysts in overall alkaline water splitting. *Electrochim. Acta* **2019,** *318*, 430-439.
5. Wei, X.; Li, N.; Liu, N., Ultrathin NiFeZn-MOF nanosheets containing few metal oxide nanoparticles grown on nickel foam for efficient oxygen evolution reaction of electrocatalytic water splitting. *Electrochim. Acta* **2019,** *318*, 957-965.
6. Dang, W.-J.; Shen, Y.-Q.; Lin, M.; Jiao, H.; Xu, L.; Wang, Z.-L., Noble-metal-free electrocatalyst based on a mixed CoNi metal-organic framework for oxygen evolution reaction. *J. Alloys Compd.* **2019,** *792*, 69-76.
7. Muthurasu, A.; Maruthapandian, V.; Kim, H. Y., Metal-organic framework derived Co3O4/MoS2 heterostructure for efficient bifunctional electrocatalysts for oxygen evolution reaction and hydrogen evolution reaction. *Appl. Catal., B* **2019,** *248*, 202-210.
8. Lin, H.-W.; Senthil Raja, D.; Chuah, X.-F.; Hsieh, C.-T.; Chen, Y.-A.; Lu, S.-Y., Bi-metallic MOFs possessing hierarchical synergistic effects as high performance electrocatalysts for overall water splitting at high current densities. *Appl. Catal., B* **2019,** *258*, 118023.
9. Senthil Raja, D.; Lin, H.-W.; Lu, S.-Y., Synergistically well-mixed MOFs grown on nickel foam as highly efficient durable bifunctional electrocatalysts for overall water splitting at high current densities. *Nano Energy* **2019,** *57*, 1-13.
10. Sun, H.; Min, Y.; Yang, W.; Lian, Y.; Lin, L.; Feng, K.; Deng, Z.; Chen, M.; Zhong, J.; Xu, L.; Peng, Y., Morphological and Electronic Tuning of Ni_2P through Iron Doping toward Highly Efficient Water Splitting. *ACS Catal.* **2019,** *9* (10), 8882-8892.
11. Zhang, X.; Liu, Q.; Shi, X.; Asiri, A. M.; Sun, X., An Fe-MOF nanosheet array with superior activity towards the alkaline oxygen evolution reaction. *Inorg. Chem. Front.* **2018,** *5* (6), 1405-1408.
12. Wang, Q.; Wei, F.; Manoj, D.; Zhang, Z.; Xiao, J.; Zhao, X.; Xiao, F.; Wang, H.; Wang, S., In situ growth of Fe(ii)-MOF-74 nanoarrays on nickel foam as an efficient electrocatalytic electrode for water oxidation: a mechanistic study on valence engineering. *Chem. Commun.* **2019,** *55* (75), 11307-11310.
13. Yang, L.; Zhu, G.; Wen, H.; Guan, X.; Sun, X.; Feng, H.; Tian, W.; Zheng, D.; Cheng, X.; Yao, Y., Constructing a highly oriented layered MOF nanoarray from a layered double hydroxide for efficient and long-lasting alkaline water oxidation electrocatalysis. *J. Mater. Chem. A,* **2019,** *7* (15), 8771-8776.
14. Ping, D.; Feng, X.; Zhang, J.; Geng, J.; Dong, X., Directed Growth of a Bimetallic MOF Membrane and the Derived NiCo Alloy@C/$Ni_xCo_{1-x}O$/Ni Foam Composite as an Efficient Electrocatalyst for the Oxygen Evolution Reaction. *ChemElectroChem* **2017,** *4* (12), 3037-3041.
15. Senthil Raja, D.; Chuah, X.-F.; Lu, S.-Y., In Situ Grown Bimetallic MOF-Based Composite as Highly Efficient Bifunctional Electrocatalyst for Overall Water Splitting with Ultrastability at High Current Densities. *Adv. Energy Mater.* **2018,** *8* (23), 1801065.
16. Rong, J.; Xu, J.; Qiu, F.; Zhu, Y.; Fang, Y.; Xu, J.; Zhang, T., Sea Urchin-Like MOF-Derived

Formation of Porous Cu_3P@C as an Efficient and Stable Electrocatalyst for Oxygen Evolution and Hydrogen Evolution Reactions. *Adv. Mater. Interfaces* **2019,** *6* (14), 1900502.
17. Sun, F.; Wang, G.; Ding, Y.; Wang, C.; Yuan, B.; Lin, Y., NiFe-Based Metal–Organic Framework Nanosheets Directly Supported on Nickel Foam Acting as Robust Electrodes for Electrochemical Oxygen Evolution Reaction. *Adv. Energy Mater.* **2018,** *8* (21), 1800584.
18. Duan, J.; Chen, S.; Zhao, C., Ultrathin metal-organic framework array for efficient electrocatalytic water splitting. *Nat. Commun.* **2017,** *8* (1), 15341.